Electric-field induced penetration of edge states at the interface between monolayer and bilayer graphene

Yasumasa Hasegawa[1] and Mahito Kohmoto[2]
[1] *Department of Material Science, Graduate School of Material Science, University of Hyogo, 3-2-1 Kouto, Kamigori, Hyogo, 678-1297, Japan*
[2] *Institute for Solid State Physics, University of Tokyo, 5-1-5 Kashiwanoha, Kashiwa, Chiba 277-8581, Japan*
(Dated: July 7, 2011, revised October 25, 2011)

The edge states in the hybrid system of single-layer and double-layer graphene are studied in the tight-binding model theoretically. The edge states in one side of the interface between single-layer and double-layer graphene are shown to penetrate into the single-layer region when the perpendicular electric field is applied, while they are localized in the double-layer region without electric field. The edge states in another side of the interface are localized in the double-layer region independent of the electric field. This field-induced penetration of the edge states can be applied to switching devices. We also find a new type of the edge states at the boundary between single-layer and the double-layer graphene.

PACS numbers: 73.22.Pr, 73.20.-r, 73.40.-c, 81.05.ue

I. INTRODUCTION

Recently, single-layer and double-layer graphene have been studied both theoretically and experimentally[1], because of the interesting properties such as the Dirac points[2,3], anomalous Hall effect[2–5], and the edge states[6–12]. The double-layer graphene has attracted peculiar interest[13] due to a band gap controlled by the electric field, which has been predicted[14,15] and observed[9,16–21].

The edge states in the single-layer graphene and double-layer graphene have been studied by many authors. In the single-layer graphene the edge states appear at the zigzag edges[6,7] and bearded edges. If the system is anisotropic, the edge states also exist at the armchair edges[8]. The edge states in the double-layer graphene has been studied[9,10,22]. The edge states at the interface between single-layer and double-layer graphene have also been studied. Transmission across the boundary has been studied theoretically using the effective-mass approximation[23–25], edge states have been studied theoretically[22,26], and quantum oscillations have been observed in the interface[27]. Vacancy-induced localized states in the multilayer graphene has been proposed[28].

In this paper we study the edge states in the hybrid system of single-layer and double-layer graphene as shown in Fig. 1. We focus on the edge states localized in the boundary between the single-layer and the double-layer regions. We obtain the new edge states localized in one side of the interface between single-layer and double-layer regions with energy $E \neq 0$. We show an interesting property that the edge states at the boundary between the single-layer and the double-layer regions penetrate into the single-layer region when the electric field is applied perpendicular to the layers.

II. MODEL

We assume zigzag edges in both the first and the second layers. Each layer has two sublattices, which we call A_1, B_1, A_2 and B_2, as shown in Fig. 1. The left part and the right part of the single-layer regions have L_{1L} and L_{1R} pairs of A_1 and B_1 sublattices in the x-direction. In the double-layer region there are L_2 quartets of (A_1, B_1, A_2, B_2) sublattices. The left edge in the left single-layer region has only B_1 sublattice, which is labeled as $n = 0$, and the right edge in the right single-layer region (A_1 sublattice) is labeled as

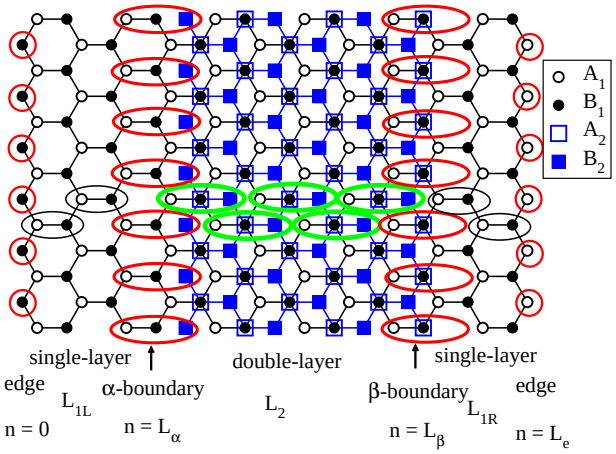

FIG. 1. (color online). Single-double-single layer graphene. Thin black ellipses are the doublets of (A_1, B_1) sites in the single-layer region, and thick green ellipses are the quartets of (A_1, B_1, A_2, B_2) sites in the double-layer region. Thick red ellipses are the triplets of (A_1, B_1, B_2) and (A_1, B_1, A_2) sites (left and right, respectively) in the boundary between single layer and double layer of the α- and β-types, respectively. Thick red circles are the zigzag edges.

$n = L_e \equiv L_{1L} + L_{1R} + L_2 + 3$. There are two boundaries between single-layer and the double-layer regions. These two boundaries are different from each other[22,24–26]. One of the boundaries has A_1, B_1 and B_2 sublattices and the other has A_1, B_1 and A_2 sublattices. We call these boundaries as α-boundary and β-boundary, respectively. The position of the α-boundary is $n = L_\alpha \equiv L_{1L}+1$, and the position of the β-boundary is $n = L_\beta \equiv L_{1L}+L_2+2$. Note that α-boundary and the β-boundary always appear as a pair if two boundaries are parallel. We assume that the left boundary is the α type and the right boundary is the β type.

We adopt the tight-binding model, where the hoppings between the nearest sites in the layer (A_1-B_1 and A_2-B_2) are taken to be t and the interlayer hoppings between the nearest sites (B_1-A_2) are taken to be $t_\perp$. We take into account the energy difference between layers (ϵ_1 and ϵ_2), which is controlled by the electric field perpendicular to the layers.

We apply the same method which we have used in studying the edge states in the single-layer graphene[8]. Imposing the periodic boundary conditions in the y direction, we can take the wave number k_y as the quantum number. For each k_y the Hamiltonian is written as a $L_{sds} \times L_{sds}$ matrix, where $L_{sds} \equiv 2L_{1L} + 4L_2 + 2L_{1R} + 8$. The eigenstates ($\Psi$) in the Schrödinger equation ($H\Psi = E\Psi$) are vectors with L_{sds} components (the wave functions for the first layer ($\Psi_{B_1,0}$, Ψ_{A_1,L_e}, Ψ_{A_1,n_1}, and Ψ_{B_1,n_1}, where $1 \le n_1 \le L_e - 1$) and the wave functions for the second layer (Ψ_{B_2,L_α}, Ψ_{A_2,L_β}, Ψ_{A_2,n_2}, and Ψ_{B_2,n_2}, where $L_\alpha + 1 \le n_2 \le L_\beta - 1$)).

In the single-layer region ($1 \le n \le L_\alpha - 1$, or $L_\beta + 1 \le n \le L_e - 1$), the Schrödinger equation is written as,

$$-2t\cos\frac{k_y}{2}\Psi_{B_1,n-1} - t\Psi_{B_1,n} = (E-\epsilon_1)\Psi_{A_1,n}, \quad (1)$$

$$-2t\cos\frac{k_y}{2}\Psi_{A_1,n+1} - t\Psi_{A_1,n} = (E-\epsilon_1)\Psi_{B_1,n}. \quad (2)$$

The equations in the region of double layer ($L_\alpha + 1 \le n \le L_\beta - 1$) are given by

$$-2t\cos\frac{k_y}{2}\Psi_{B_1,n-1} - t\Psi_{B_1,n} = (E-\epsilon_1)\Psi_{A_1,n}, \quad (3)$$

$$-2t\cos\frac{k_y}{2}\Psi_{A_1,n+1} - t\Psi_{A_1,n} - t_\perp\Psi_{A_2,n} = (E-\epsilon_1)\Psi_{B_1,n}, \quad (4)$$

$$-2t\cos\frac{k_y}{2}\Psi_{B_2,n-1} - t\Psi_{B_2,n} - t_\perp\Psi_{B_1,n} = (E-\epsilon_2)\Psi_{A_2,n}, \quad (5)$$

$$-2t\cos\frac{k_y}{2}\Psi_{A_2,n+1} - t\Psi_{A_2,n} = (E-\epsilon_2)\Psi_{B_2,n}. \quad (6)$$

At the left edge of the single-layer region we obtain the equation to be Eq. (2) with $n = 0$ and $\Psi_{A_1,0} = 0$, since there are no A_1 sublattice at the left edge in the single-layer region, i.e.,

$$-2t\cos\frac{k_y}{2}\Psi_{A_1,1} = (E-\epsilon_1)\Psi_{B_1,0}. \quad (7)$$

Similarly, we obtain the equation at the right edge of the single-layer region to be Eq. (1) with $n = L_e$ and $\Psi_{B_1,L_e} = 0$,

$$-2t\cos\frac{k_y}{2}\Psi_{B_1,L_e-1} = (E-\epsilon_1)\Psi_{A_1,L_e}, \quad (8)$$

At the α-boundary, the equations are obtained by taking $n = L_\alpha$ and $\Psi_{A_2,L_\alpha} = 0$ in Eqs. (3), (4), and (6), since there are no A_2 sublattices at the α-boundary.

$$-2t\cos\frac{k_y}{2}\Psi_{B_1,L_\alpha-1} - t\Psi_{B_1,L_\alpha} = (E-\epsilon_1)\Psi_{A_1,L_\alpha}, \quad (9)$$

$$-2t\cos\frac{k_y}{2}\Psi_{A_1,L_\alpha+1} - t\Psi_{A_1,L_\alpha} = (E-\epsilon_1)\Psi_{B_1,L_\alpha}, \quad (10)$$

$$-2t\cos\frac{k_y}{2}\Psi_{A_2,L_\alpha+1} = (E-\epsilon_2)\Psi_{B_2,L_\alpha}. \quad (11)$$

The equations at the β-boundary are obtained by taking $n = L_\beta$ and $\Psi_{B_2,L_\beta} = 0$, in Eqs. (3), (4), and (5). Explicitly, the equations at the β-boundary are given by

$$-2t\cos\frac{k_y}{2}\Psi_{B_1,L_\beta-1} - t\Psi_{B_1,L_\beta} = (E-\epsilon_1)\Psi_{A_1,L_\beta}, \quad (12)$$

$$-2t\cos\frac{k_y}{2}\Psi_{A_1,L_\beta+1} - t\Psi_{A_1,L_\beta} - t_\perp\Psi_{A_2,L_\beta} = (E-\epsilon_1)\Psi_{B_1,L_\beta}, \quad (13)$$

$$-2t\cos\frac{k_y}{2}\Psi_{B_2,L_\beta-1} - t_\perp\Psi_{B_1,L_\beta} = (E-\epsilon_2)\Psi_{A_2,L_\beta}. \quad (14)$$

By taking $E = \epsilon_1$, we obtain that Eqs. (1) and (2) are two independent equations for $\Psi_{B_1,n}$ and $\Psi_{A_1,n}$, respectively, in the single-layer regions. When $\epsilon_1 = \epsilon_2 = 0$, Eqs. (3) - (6) become two sets of coupled equations for ($\Psi_{A_1,n}$, $\Psi_{A_2,n}$) and ($\Psi_{B_1,n}$, $\Psi_{B_2,n}$) in the double-layer region by taking $E = 0$. However, if $\epsilon_1 \neq \epsilon_2$, these equations cannot be separated into the independent equations for any E. This is the origin of the field-induced penetration of the edge states into the first-layer region at the β-boundary, as we will show below.

III. STRICTLY LOCALIZED STATES AT $k_y = \pi$

Since $\cos k_y/2 = 0$ at $k_y = \pi$, Eqs. (1) - (14) are the equations within the same group of n, i.e. the states at $k_y = \pi$ are strictly localized at the ellipses or circles in Fig. 1, as in the single-layer graphene[8].

The energies at $k_y = \pi$ in the single-layer regions are obtained from Eqs (1) and (2), as

$$E_{s,\pm} = \pm t + \epsilon_1, \quad (15)$$

with $(L_{1L} + L_{1R})$-fold degeneracy. The energies of the strictly localized states in the double-layer region are ob-

tained as the eigenvalues of the matrix

$$M_d = \begin{pmatrix} \epsilon_1 & -t & 0 & 0 \\ -t & \epsilon_1 & -t_\perp & 0 \\ 0 & -t_\perp & \epsilon_2 & -t \\ 0 & 0 & -t & \epsilon_2 \end{pmatrix}, \tag{16}$$

and they are obtained to be

$$E_{d,\pm,\pm} = \frac{\epsilon_1+\epsilon_2}{2} \pm \sqrt{(\frac{\Delta\epsilon}{2})^2 + t^2 + \frac{t_\perp^2}{2} \pm \sqrt{(\Delta\epsilon)^2 t^2 + t^2 t_\perp^2 + \frac{t_\perp^4}{4}}}, \tag{17}$$

where $\Delta\epsilon = \epsilon_1 - \epsilon_2$, with L_2-fold degeneracy.

At the left and the right edges we obtain the energy as

$$E_L = E_R = \epsilon_1. \tag{18}$$

At the α-boundary we obtain the energies of the strictly localized states as the eigenvalues of the matrix

$$M_\alpha = \begin{pmatrix} \epsilon_1 & -t & 0 \\ -t & \epsilon_1 & 0 \\ 0 & 0 & \epsilon_2 \end{pmatrix}, \tag{19}$$

which are obtained as

$$E_{\alpha,0} = \epsilon_2, \tag{20}$$

and

$$E_{\alpha,\pm} = \pm t + \epsilon_1. \tag{21}$$

The energies of the strictly localized states at the β-boundary are obtained as the eigenvalues of the matrix,

$$M_\beta = \begin{pmatrix} \epsilon_1 & -t & 0 \\ -t & \epsilon_1 & -t_\perp \\ 0 & -t_\perp & \epsilon_2 \end{pmatrix}. \tag{22}$$

When $|\epsilon_1| \ll t$ and $|\epsilon_2| \ll t$, we obtain the energies as

$$E_{\beta 0} = \epsilon_2 + \frac{t_\perp^2}{t^2+t_\perp^2}\Delta\epsilon + \frac{t^4 t_\perp^2}{(t^2+t_\perp^2)^4}(\Delta\epsilon)^3 + O((\Delta\epsilon)^5) \tag{23}$$

$$E_{\beta\pm} = \pm\sqrt{t^2+t_\perp^2} + \epsilon_2 + \frac{(2t^2+t_\perp^2)}{2(t^2+t_\perp^2)}\Delta\epsilon \pm \frac{t_\perp^2(4t^2+t_\perp^2)}{8(t^2+t_\perp^2)^{5/2}}(\Delta\epsilon)^2 + O((\Delta\epsilon)^3). \tag{24}$$

The eigenstates with the eigenvalues $E_{\beta,0}$ and $E_{\beta,\pm}$ are obtained as

$$\begin{pmatrix} \Psi_{A_1,L_\beta} \\ \Psi_{B_1,L_\beta} \\ \Psi_{A_2,L_\beta} \end{pmatrix} = \Psi_{A_2,L_\beta} \begin{pmatrix} -\frac{t_\perp}{t} + O((\Delta\epsilon)^2)) \\ -\frac{t_\perp\Delta\epsilon}{t^2+t_\perp^2} + O((\Delta\epsilon)^3)) \\ 1 \end{pmatrix}, \tag{25}$$

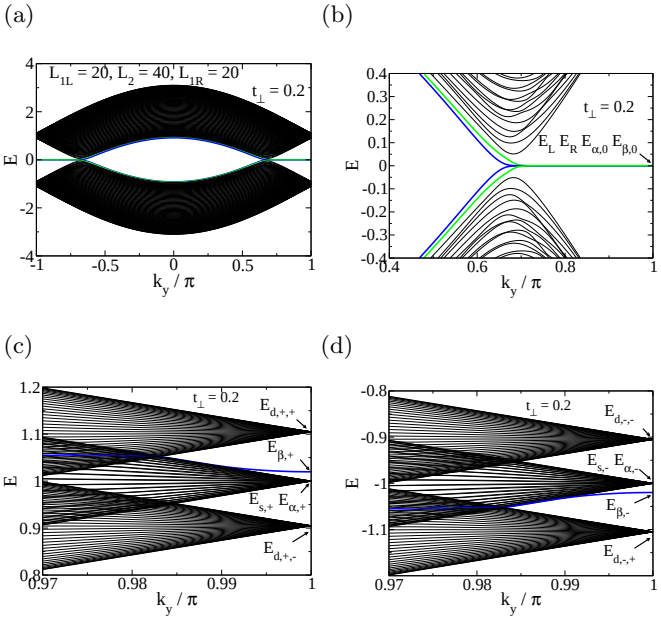

FIG. 2. (color online). Energy as a function of k_y for single-double-single graphene. There are four edge states at $E = 0$ as shown in (b), two of them are edge states at the left and the right zigzag edges of single-layer regions (see Fig. 3 (a)). The other two edge states at $E = 0$ are the edge states in the double-layer region at the α and the β boundaries (see Fig. 3 (b) and (c)). There exist other two edge states at $E = E_{\beta,+}$ and $E = E_{\beta,-}$ near $|k_y| = \pi$ as shown in (c) and (d).

and

$$\begin{pmatrix} \Psi_{A_1,L_\beta} \\ \Psi_{B_1,L_\beta} \\ \Psi_{A_2,L_\beta} \end{pmatrix} = \Psi_{A_1,L_\beta} \begin{pmatrix} 1 \\ \mp\frac{\sqrt{t^2+t_\perp^2}}{t} + \frac{t_\perp^2\Delta\epsilon}{2t(t^2+t_\perp^2)} + O((\Delta\epsilon)^2)) \\ \frac{t_\perp}{t} \mp \frac{t_\perp\Delta\epsilon}{t\sqrt{t^2+t_\perp^2}} + O((\Delta\epsilon)^2)) \end{pmatrix}, \tag{26}$$

respectively.

Since E_L, E_R, $E_{\alpha,0}$, $E_{\beta,0}$, and $E_{\beta,\pm}$ are different from the energies of the macroscopically degenerate states ($E_{s,\pm}$ and $E_{d,\pm,\pm}$), the eigenstates with these energies become the well-defined edge states at $k_y \approx \pi$, as we will show below.

IV. EDGE STATES WITHOUT PERPENDICULAR ELECTRIC FIELD

A. edge states with $E = 0$

First, we study the edge states in the case of no external electric field ($\epsilon_1 = \epsilon_2 = 0$). We plot the energy as a function of k_y in Fig. 2, where we take $t = 1$, $t_\perp = 0.2$, $L_{1L} = 20$, $L_{1R} = 20$, $L_2 = 40$, and $\epsilon_1 = \epsilon_2 = 0$. As shown

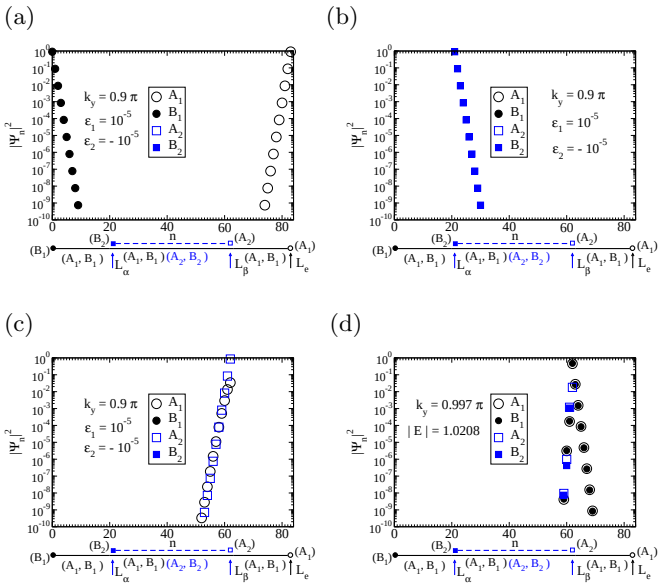

FIG. 3. (color online). Edge states localized (a) at the left and the right edges, (b) at the α-boundary and (c) at the β-boundary at $E = 0$ and $k_y = 0.9\pi$. (d) is the edge state localized at the β-boundary at $E \approx E_{\beta,+}$ or $E \approx E_{\beta,-}$ and $k_y = 0.997\pi$.

in the previous section, there are four states which have $E = 0$ when $\epsilon_1 = \epsilon_2 = 0$ and $k_y = \pi$, i.e., E_L, E_R, $E_{\alpha,0}$, and $E_{\beta,0}$. Two of them are edge states localized at each edge in the single-layer regions ($n = 0$ and $n = L_e$) for $|k_y| > 2\pi/3$, same as the single-layer graphene[8]. The edge state localized at the left edge of the single layer is given by

$$\Psi_{B_1,n} = \left(-2\cos\frac{k_y}{2}\right)^n \Psi_{B_1,0}, \tag{27}$$

where $0 \le n \le L_{1L}$ and other components of Ψ are zero. The edge state localized at the right edge of the single layer is given by

$$\Psi_{A_1,L_e-j} = \left(-2\cos\frac{k_y}{2}\right)^j \Psi_{A_1,L_e}, \tag{28}$$

where $0 \le j \le L_{1R}$ and other components of Ψ are zero.

The other edge states with $E = 0$ are localized at the α and β boundaries. As shown in Appendix A, the edge state localized at the α-boundary are obtained as

$$\begin{pmatrix} \Psi_{B_1,L_\alpha+j} \\ \Psi_{B_2,L_\alpha+j} \end{pmatrix} = \begin{pmatrix} 0 \\ \left(-2\cos\frac{k_y}{2}\right)^j \Psi_{B_2,L_\alpha} \end{pmatrix}, \tag{29}$$

where $0 \le j \le L_2$ and other components of Ψ are zero. The edge states at the β boundary are obtained as

$$\begin{pmatrix} \Psi_{A_1,L_\beta-j} \\ \Psi_{A_2,L_\beta-j} \end{pmatrix} = \left(-2\cos\frac{k_y}{2}\right)^j \Psi_{A_2,L_\beta} \begin{pmatrix} -\frac{t_\perp}{t}(1+j) \\ 1 \end{pmatrix}, \tag{30}$$

where $0 \le j \le L_2$ and other components of Ψ are zero.

These results are consistent with the results obtained in the bilayer edge[10] and the graphite steps[22]. The edge state at the β-boundary has the finite amplitudes of the wave functions at A_1 and A_2 sites, while that at the α-boundary has the finite amplitude only at the B_2 sites.

We plot the square of the absolute value of the wave functions in Figs. 3 (a), (b) and (c), in which we have taken $\epsilon_1 = 10^{-5}$ and $\epsilon_2 = -10^{-5}$ in order to lift the degeneracy of the edge states. We plot two edge states together in Fig. 3 (a), which are localized in the left and the right edges of the single-layer regions. There exist two localized states at each boundary between single-layer and double-layer, as shown in Fig. 3 (b) and (c).

B. edge states with $E \neq 0$

At the β-boundary there exist other edge states, which have energy $E \approx E_{\beta,\pm}$ at $|k_y| \approx \pi$. In Fig. 3 (d) we plot the amplitudes of the wave functions of the edge states at $k_y = 0.997\pi$ and $E \approx E_{\beta,+}$. Note that if $\{\Psi_{A_1,n_1}, \Psi_{B_1,n_1}, \Psi_{A_2,n_2}, \Psi_{B_2,n_2}\}$ is the eigenstate with energy E, $\{\Psi_{A_1,n_1}, -\Psi_{B_1,n_1}, \Psi_{A_2,n_2}, -\Psi_{B_2,n_2}\}$ is also the eigenstate with energy $-E$, when $\epsilon_1 = \epsilon_2 = 0$. Therefore, $|\Psi_{A_1,n}|^2$, $|\Psi_{B_1,n}|^2$ $|\Psi_{A_2,n}|^2$, and $|\Psi_{B_2,n}|^2$ for the edge states with $E \approx E_{\beta,-} = -E_{\beta,+}$ are the same as these with $E \approx E_{\beta,+}$.

As seen in Fig. 2 (c) and (d), the edge states at $E \approx E_{\beta,\pm}$ exist at $|k_y| \approx \pi$. Although the bulk extended states with the same energy $E \approx E_{\beta,\pm}$ also exist at other values of k_y, the density of states has a peak at that energy due to the edge states. Therefore, the edge states can be observed as a peak in the differential conductance (dI/dV) by the spatially resolving scanning tunneling spectroscopy (STS)[11,12] at the β-boundary.

These edge states at $E \approx E_{\beta,\pm}$ can be understood by considering the equations in the single-layer regions Eqs. (1) and (2) (see Appendix B).

The existence of these edge states has not been known before, as far as we know. Although the existence of the edge states at $E \neq 0$ has been suggested as a perfectly reflecting states by Nakanishi et al.[24], the pure edge states are obtained only at $E = 0$ in their paper, since they adopted the effective-mass scheme, which can be used only near the Dirac points.

V. EDGE STATES IN THE PRESENCE OF PERPENDICULAR ELECTRIC FIELD

In this section we study the edge states in the presence of perpendicular electric field. When the electric field is applied perpendicular to the layers, the potential difference between the first and the second layers, $(\epsilon_1 - \epsilon_2)$, becomes finite. Even in that case we have the edge states at the left and right edges in the single-layer regions, which are given by $E = \epsilon_1$, $\Psi_{A_2,n} = \Psi_{B_2,n} = 0$

and $\Psi_{A_1,n} = 0$ (the edge states at the left edge) or $\Psi_{B_1,n} = 0$ (the edge states at the right edge). The edge states at the α-boundary, which are given by $E = \epsilon_2$ and $\Psi_{A_1,n} = \Psi_{B_1,n} = \Psi_{A_2,n} = 0$ are also not affected by the perpendicular electric field, since the edge states at the α-boundary is localized only in the second layer. As seen in Fig. 4 (a) and (b), the states with $E = E_L = E_R = \epsilon_1$ and $E = E_{\alpha,0} = \epsilon_2$ exist for $|k_y| \gtrsim 2\pi/3$ even when they are in the upper or lower band.

The edge states at the β-boundary, however, is changed drastically by the perpendicular electric field and they are quite different from the edge states in the bilayer graphene[10].

We study the edge states at the β-boundary with the energy $E \approx E_{\beta,0}$ at $k_y \approx \pi$ in the perpendicular electric field in the similar method given in Appendix B.

We study the single-layer region near the β-boundary. We assume that the energy difference between the first and second layers, $\epsilon_1 - \epsilon_2$ is smaller than the hopping energy in the plane, t. Then we obtain

$$|e_0| = \left|\frac{E-\epsilon_1}{t}\right| \approx \left|\frac{t(\epsilon_2-\epsilon_1)}{t^2+t_\perp^2}\right| < 1, \tag{31}$$

when $E \approx E_{\beta,0}$. The eigenvalues ($\lambda_\pm$) of the matrix T (Eq. (B5)) in the right single layer-region ($L_\beta + 1 \le n \le L_e - 1$) are real when

$$|a| < |1 - |e_0|| = 1 - |e_0|, \tag{32}$$

where $a = -\cos(k_y/2)$ as discussed in Appendix B. We expand $\lambda_\pm$ and V (defined in Eqs. (B7) and (B8)) in a, and we obtain

$$\lambda_+ \approx \frac{1-e_0^2}{a} > 1, \tag{33}$$

$$\lambda_- \approx \frac{a}{1-e_0^2} < 1, \tag{34}$$

and

$$V \approx \begin{pmatrix} 2 & -2e_0 \\ -2e_0 & 2 \end{pmatrix}. \tag{35}$$

Therefore, the eigenvector of T with the eigenvalue λ_- is the edge state localized at the β-boundary given by

$$\begin{pmatrix} \Psi_{A_1,L_\beta+1+j} \\ \Psi_{B_1,L_\beta+1+j} \end{pmatrix} = \lambda_-^j \Psi_{B_1,L_\beta+1} \begin{pmatrix} -\frac{2e_0}{\sqrt{D}-a^2+e_0^2+1} \\ 1 \end{pmatrix} \approx \lambda_-^j \Psi_{B_1,L_\beta+1} \begin{pmatrix} -e_0 \\ 1 \end{pmatrix}, \tag{36}$$

where $0 \le j \le L_{1R}$.

If $\Delta\epsilon = 0$, we obtain $\Psi_{B_1,L_\beta} = 0$ from Eq. (25) and we obtain $\Psi_{A_1,L_\beta+1} = \Psi_{B_1,L_\beta+1} = 0$ from Eq. (B24). In this case, Eq. (36) shows that the edge states with $E = E_{\beta,0} = 0$ and $|2\cos(k_y/2)| < 1$ is localized only in the double-layer region at the β-boundary, if $\Delta\epsilon = 0$, as shown Fig. 3(c).

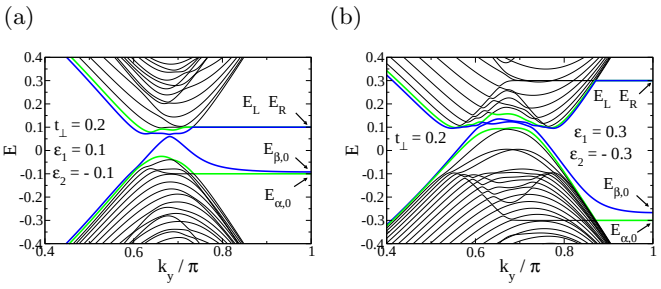

FIG. 4. (color online). Energy of single-double-single layer graphene as a function of k_y with different site energy in each layers ((a):$\epsilon_1 = -\epsilon_2 = 0.1 < t_\perp$ and (b):$\epsilon_1 = -\epsilon_2 = 0.3 > t_\perp$.).

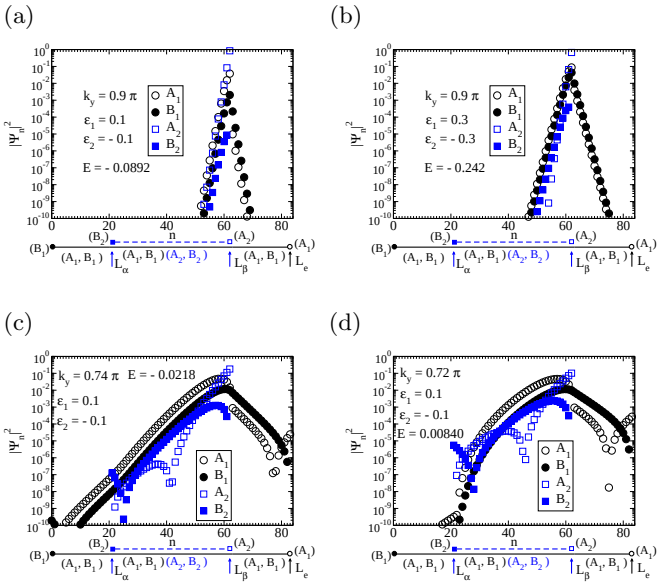

FIG. 5. (color online). Edge states at the β-boundary in single-double-single layer graphene at $k_y = 0.9\pi$ with $\epsilon_1 = -\epsilon_2 = 0.1$, (a) and 0.3 (b). The localization length of the edge states becomes large when k_y approaches to $2\pi/3$. The edge states with $\epsilon_1 = -\epsilon_2 = 0.1$ at $k_y = 0.74\pi$ (c) and $k_y = 0.72\pi$ (d) are shown.

If $\Delta\epsilon \neq 0$ due to the perpendicular electric field, Ψ_{B_1,L_β} and $\Psi_{B_1,L_\beta+1}$ become finite for the edge states at the β-boundary, resulting in the penetration of the edge states into the single-layer region.

In this way the strictly localized state at the β-boundary at $k_y = \pi$ ($a = 0$) and $E = E_{\beta,0}$ becomes the localized states which have the finite amplitudes both in the single-layer and double-layer regions when $|2\cos k_y/2| < 1 - |e_0|$. In Fig. 4 we plot the energy as a function of k_y in the case of the finite energy difference between the first layer and the second layer. The energy of the edge states at the β-boundary depends on k_y as shown in Fig. 4. In Fig. 5 (a) and (b) we plot the wave functions of the edge states at $E \approx E_{\beta,0}$ and

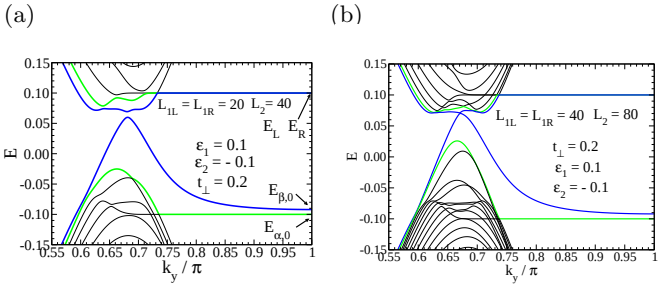

FIG. 6. (color online). Energy of single-double-single layer graphene as a function of k_y with different site energy in each layers ($\epsilon_1 = -\epsilon_2 = 0.1 < t_\perp$). Two systems with different width ($L_{1L} = L_{1R} = 20$, $L_2 = 40$ (a) and $L_{1L} = L_{1R} = 40$, $L_2 = 80$ (b)) are shown. The narrower system (a) is the same but a close up of Fig. 4. The bulk energy gap (the gap between the upper blue line and lower green line at $k_y \approx 2\pi/3$) becomes smaller as the width of the system becomes wider. There exists a small energy gap at $k_y \approx 2\pi/3$ between two blue lines in (a), because the localization length of the edge state at the β edge becomes comparable to the width of the system. For the wider system (b), the energy gap between two blue lines becomes negligible.

$k_y = 0.9\pi$ for $\epsilon_1 = -\epsilon_2 = 0.1$ and 0.3. In contract to the case of $\epsilon_1 = \epsilon_2 = 0$ (Fig. 3 (c)), all components of the wave functions are finite in the double-layer region at the β-boundary ($n \leq L_\beta$). The wave function has finite amplitudes also in the single-layer region ($n \geq L_\beta + 1$), which means the penetration of the edge state at the β-boundary is induced by the electric field. When k_y approaches to $2\pi/3$, the energy of the edge states (the lower blue line) deviates from $E_{\beta,0}$, as seen in Fig. 4. The localization length of the edge states becomes large as k_y approaches to $2\pi/3$ (see Fig. 5 (c) and (d)). The effects of the α-boundary ($n = L_\alpha$) and the right edge ($n = L_e$) on the edge state at β-boundary are seen in Fig. 5 (c) and (d).

We mention the bulk energy gap caused by the perpendicular electric field. Though the bulk energy gap is originated in the double-layer region, the system with finite width of the single-layer regions in both side as shown in Fig.1 has the bulk energy gap, since the the states except for the edge states are extended in both single-layer and double-layer regions. When the widths of the single-layer regions become larger, the bulk energy gap becomes smaller, as shown in Fig. 6 (a) and (b), which show the k_y-dependences of the energies for the systems with different width. Therefore, the critical value of k_y, at which the edge state at the β-boundary has the energy between the bulk energy gap, depends on the width of the system. The edge states at $k_y = 0.74\pi$ and 0.72π (Fig. 5 (c) and (d)) have energies between bulk gap ($-0.0252 < E < 0.693$) for the system with $L_{1L} = L_{1R} = 20$ and $L_2 = 40$, while the edge states at $k_y = 0.9\pi$ (Fig. 5 (a)) has the energy outside of the bulk gap. Since STS probes the local density of states[11,12], the edge states can be observed even if they are outside of the bulk gap. Therefore, the field-induced penetration of the edge state into the single-layer region can be observed by STS.

As shown in Fig. 4 (a), Fig. 6 (a) and (b), the edge states at the β-boundary have energies in the bulk energy gap at $|k_y| \gtrsim 2\pi/3$ if $|\epsilon_1 - \epsilon_2| \lesssim 2t_\perp$. In this case, the edge states are partially filled in the less than half-filled systems. Then electric current flow along the β-boundary (y direction) in both single-layer region and double-layer region (see Fig. 5 (a), (c), and (d)). The edge states are partially filled even when the perpendicular electric field is not applied. However, the contribution of the edge states at the β-boundary to the electric current is only in the double-layer region in the absence of the perpendicular electric field, since the edge states are localized only in the double-layer region of the β-boundary (see Fig. 3 (c)). Thus, the electric conductivity along the β-boundary in the single-layer region at the β-boundary is increased by the perpendicular electric field.

VI. CONCLUSION

We have studied the edge states in the hybrid system of the single-layer and double-layer graphene. By using the tight-binding model, we obtain the analytic solution of the edge states at the boundary between single-layer and double-layer regions when perpendicular electric field is not applied. We found that the edge states at the α-boundary are localized only in the second layer, and the edge states at the β-boundary have finite amplitude in both layers in the double-layer region.

We also find the new edge states with $E \approx E_{\beta,\pm}$, which are localized at the β-boundary.

When the perpendicular electric field is applied, the edge states at the β-boundary are shown to change drastically. The edge states at the β-boundary have finite amplitudes at all sites in both regions of the boundary. The penetration of the edge states induced by the electric field can be observed experimentally by STS[11,12]. The bulk gap becomes smaller for the systems with the wider width of the single-layer regions. The edge states, however, are possible to be observed by STS even though the energy of the edge states are not located in the middle of the bulk gap because the edge states has larger amplitudes of the wave functions than that for the extended states with the same energy in the region near the boundary.

We propose a simple method to observe the electric-field-induced penetration of the edge states. The conductivity between two terminals placed at the single-layer region at the β-boundary will become large when the perpendicular electric field is applied, as the edge states at the β-boundary penetrate into the single-layer region. This electric-field-induced penetration of the edge states can be used as electrical devices.

Appendix A: analytical solutions for the edge states with $E = 0$ at the α and β boundaries when $\epsilon_1 = \epsilon_2$

The equations in the double-layer region ((3) - (6)) are decoupled into two groups, when $\epsilon_1 = \epsilon_2 = 0$ and $E = 0$. Eqs. (3) and (5) are written as

$$\begin{pmatrix} 1 & 0 \\ \frac{t_\perp}{t} & 1 \end{pmatrix} \begin{pmatrix} \Psi_{B_1,n} \\ \Psi_{B_2,n} \end{pmatrix} = \left(-2\cos\frac{k_y}{2}\right) \begin{pmatrix} \Psi_{B_1,n-1} \\ \Psi_{B_2,n-1} \end{pmatrix}, \tag{A1}$$

where $L_\alpha + 1 \le n \le L_\beta - 1$. From this equation we obtain

$$\begin{pmatrix} \Psi_{B_1,L_\alpha+j} \\ \Psi_{B_2,L_\alpha+j} \end{pmatrix} = \left(-2\cos\frac{k_y}{2}\right)^j \begin{pmatrix} 1 & 0 \\ -\frac{t_\perp}{t}j & 1 \end{pmatrix} \begin{pmatrix} \Psi_{B_1,L_\alpha} \\ \Psi_{B_2,L_\alpha} \end{pmatrix}, \tag{A2}$$

where $0 \le j \le L_2$. Since we obtain

$$\Psi_{B_1,L_\alpha} = \left(-2\cos\frac{k_y}{2}\right)^{L_\alpha} \Psi_{B_1,0}, \tag{A3}$$

from the equations in the single-layer region (Eq. (1)), we can take $\Psi_{B_1,L_\alpha} = 0$ for $|2\cos(k_y/2)| < 1$ and $L_\alpha \gg 1$. Therefore, the edge state localized at the α-boundary are obtained as

$$\begin{pmatrix} \Psi_{B_1,L_\alpha+j} \\ \Psi_{B_2,L_\alpha+j} \end{pmatrix} = \begin{pmatrix} 0 \\ \left(-2\cos\frac{k_y}{2}\right)^j \Psi_{B_2,L_\alpha} \end{pmatrix}, \tag{A4}$$

where $0 \le j \le L_2$ and other components of Ψ are zero.

In the same way we obtain from equations (4) and (6),

$$\begin{pmatrix} \Psi_{A_1,L_\beta-j} \\ \Psi_{A_2,L_\beta-j} \end{pmatrix} = \left(-2\cos\frac{k_y}{2}\right)^j \begin{pmatrix} 1 & -\frac{t_\perp}{t}j \\ 0 & 1 \end{pmatrix} \begin{pmatrix} \Psi_{A_1,L_\beta} \\ \Psi_{A_2,L_\beta} \end{pmatrix}, \tag{A5}$$

where $0 \le j \le L_2$. As in the edge state in the α-boundary, we can take $\Psi_{A_1,L_\beta+1} = 0$, when $|2\cos(k_y/2)| < 1$ and $L_{1R} \gg 1$. Then we obtain from Eq. (13)

$$\Psi_{A_1,L_\beta} = -\frac{t_\perp}{t}\Psi_{A_2,L_\beta}, \tag{A6}$$

and we obtain the edge state at the β-boundary as

$$\begin{pmatrix} \Psi_{A_1,L_\beta-j} \\ \Psi_{A_2,L_\beta-j} \end{pmatrix} = \left(-2\cos\frac{k_y}{2}\right)^j \Psi_{A_2,L_\beta} \begin{pmatrix} -\frac{t_\perp}{t}(1+j) \\ 1 \end{pmatrix}, \tag{A7}$$

where $0 \le j \le L_2$ and other components of Ψ are zero.

Appendix B: analytical solutions for the edge states with $E \approx E_{\beta,\pm}$ at the β boundary

By replacing n by $n+1$ in Eq. (1), we can write the equations in the single-layer regions, Eqs. (1) and (2), as

$$\begin{pmatrix} e_0 & 1 \\ a & 0 \end{pmatrix} \begin{pmatrix} \Psi_{A_1,n+1} \\ \Psi_{B_1,n+1} \end{pmatrix} = \begin{pmatrix} 0 & a \\ 1 & e_0 \end{pmatrix} \begin{pmatrix} \Psi_{A_1,n} \\ \Psi_{B_1,n} \end{pmatrix}, \tag{B1}$$

where

$$a = -2\cos\frac{k_y}{2}, \tag{B2}$$

$$e_0 = \frac{E - \epsilon_1}{t}. \tag{B3}$$

In Eq. (B1), we can take $0 \le n \le L_\alpha$ or $L_\beta + 1 \le n \le L_e - 1$, and $\Psi_{A_1,0} = \Psi_{B_1,L_e} = 0$. Then we obtain

$$\begin{pmatrix} \Psi_{A_1,n+1} \\ \Psi_{B_1,n+1} \end{pmatrix} = T \begin{pmatrix} \Psi_{A_1,n} \\ \Psi_{B_1,n} \end{pmatrix}, \tag{B4}$$

where T is a 2×2 matrix given by

$$T = \begin{pmatrix} \frac{1}{a} & \frac{e_0}{a} \\ -\frac{e_0}{a} & \frac{a^2 - e_0^2}{a} \end{pmatrix}. \tag{B5}$$

If $e_0 \neq 0$, the matrix T is diagonalized by the matrix V as

$$V^{-1}TV = \begin{pmatrix} \lambda_+ & 0 \\ 0 & \lambda_- \end{pmatrix}, \tag{B6}$$

where $\lambda_\pm$ are the eigenvalues of the matrix T,

$$\lambda_\pm = \frac{1}{2a}\left(a^2 - e_0^2 + 1 \pm \sqrt{D}\right), \tag{B7}$$

$$V = \begin{pmatrix} \sqrt{D} - a^2 + e_0^2 + 1 & -2e_0 \\ -2e_0 & \sqrt{D} - a^2 + e_0^2 + 1 \end{pmatrix}, \tag{B8}$$

$$V^{-1} = \frac{1}{C}\begin{pmatrix} \sqrt{D} - a^2 + e_0^2 + 1 & 2e_0 \\ 2e_0 & \sqrt{D} - a^2 + e_0^2 + 1 \end{pmatrix}, \tag{B9}$$

$$C = 2\sqrt{D}\left(\sqrt{D} - a^2 + e_0^2 + 1\right), \tag{B10}$$

and

$$D = (a+e_0+1)(a-e_0+1)(a+e_0-1)(a-e_0-1). \tag{B11}$$

Note that

$$\lambda_+\lambda_- = 1. \tag{B12}$$

If $D < 0$, $\lambda_- = \lambda_+^*$ and $|\lambda_+| = |\lambda_-| = 1$. In this case we obtain the extended states, if the boundary conditions at $n = 0$, L_α, L_β, and L_e are satisfied. On the other hand, if $D > 0$, two eigenvalues of T are real and either $|\lambda_+|$ or $|\lambda_-|$ is smaller than 1. In this case $|\Psi_{A_1,L_\beta+j}|$ and $|\Psi_{B_1,L_\beta+j}|$ can decrease as $|\lambda_+|^j$ $|\lambda_-|^j$ obtained from Eq. B4, if the boundary conditions at $n = L_\beta$ are satisfied by the corresponding eigenstate of T. Note that $D > 0$ is obtained if and only if

$$||a| - |e_0|| > 1. \tag{B13}$$

Now we examine the edge states at the β-boundary with $E \approx E_{\beta,\pm}$. When $k_y \approx \pi$ and $E \approx E_{\beta,\pm} = \pm\sqrt{t^2+t_\perp^2}$, we obtain

$$|a| \ll 1 \tag{B14}$$

and

$$|e_0| \approx \sqrt{1+\left(\frac{t_\perp}{t}\right)^2} > 1. \tag{B15}$$

Then the inequality Eq. (B13) is satisfied and the edge states can exist. In order to examine the edge states with $E \approx E_{\beta,\pm}$, we expand D, $\lambda_\pm$ and V in a when $|a| < |e_0| - 1$, as

$$D \approx (e_0^2-1)^2 - 2(e_0^2+1)a^2, \tag{B16}$$

$$\lambda_+ \approx -\frac{a}{e_0^2-1}, \tag{B17}$$

$$\lambda_- \approx -\frac{e_0^2-1}{a}, \tag{B18}$$

and

$$V \approx (-2e_0)\begin{pmatrix} -e_0 & 1 \\ 1 & -e_0 \end{pmatrix}. \tag{B19}$$

In this case $\lambda_\pm$ are real and

$$|\lambda_+| < 1 < |\lambda_-|. \tag{B20}$$

The eigenvector of the matrix T with the eigenvalue λ_+ is given by the first column of matrix V. Therefore, when $\Psi_{A,L_\beta+1}$ and $\Psi_{B,L_\beta+1}$ $(0 \le j \le L_{1R})$ satisfy the equation,

$$\frac{\Psi_{A_1,L_\beta+1}}{\Psi_{B_1,L_\beta+1}} = -\frac{\sqrt{D}-a^2+e_0^2+1}{2e_0}, \tag{B21}$$

we obtain from Eq. B4

$$\begin{aligned}\begin{pmatrix} \Psi_{A_1,L_\beta+1+j} \\ \Psi_{B_1,L_\beta+1+j} \end{pmatrix} &= \lambda_+^j \Psi_{B_1,L_\beta+1}\begin{pmatrix} -\frac{\sqrt{D}-a^2+e_0^2+1}{2e_0} \\ 1 \end{pmatrix} \\ &\approx \lambda_+^j \Psi_{B_1,L_\beta+1}\begin{pmatrix} -e_0 \\ 1 \end{pmatrix},\end{aligned} \tag{B22}$$

where $0 \le j \le L_{1R}$. This state is the edge state localized at the β-boundary.

At the β-boundary the equations for Ψ_{A_1,L_β}, Ψ_{B_1,L_β}, Ψ_{A_2,L_β}, $\Psi_{A_1,L_\beta+1}$, and $\Psi_{B_1,L_\beta+1}$ are obtained from Eq. (1) with $n = L_\beta + 1$ and Eq. (13),

$$\begin{pmatrix} e_0 & 1 \\ a & 0 \end{pmatrix}\begin{pmatrix} \Psi_{A_1,L_\beta+1} \\ \Psi_{B_1,L_\beta+1} \end{pmatrix} = \begin{pmatrix} 0 & a & 0 \\ 1 & e_0 & \frac{t_\perp}{t} \end{pmatrix}\begin{pmatrix} \Psi_{A_1,L_\beta} \\ \Psi_{B_1,L_\beta} \\ \Psi_{A_2,L_\beta} \end{pmatrix}. \tag{B23}$$

This equation is written as

$$\begin{pmatrix} \Psi_{A_1,L_\beta+1} \\ \Psi_{B_1,L_\beta+1} \end{pmatrix} = \begin{pmatrix} \frac{1}{a} & \frac{e_0}{a} & \frac{t_\perp}{at} \\ -\frac{e_0}{a} & \frac{a^2-e_0^2}{a} & -\frac{e_0 t_\perp}{at} \end{pmatrix}\begin{pmatrix} \Psi_{A_1,L_\beta} \\ \Psi_{B_1,L_\beta} \\ \Psi_{A_2,L_\beta} \end{pmatrix}. \tag{B24}$$

This boundary condition as well as the condition that the wave functions should decrease exponentially in the double-layer region in the left part (the double-layer region) of the β-boundary can be satisfied by adjusting e_0, Ψ_{A_1,L_β}, Ψ_{B_1,L_β}, and Ψ_{A_2,L_β}. It is indeed possible as seen in Fig. 3(d). These edge states at $E \approx E_{\beta,\pm}$ are localized at the β-boundary and the wave functions have the finite amplitudes in both sides (both single-layer and double-layer regions) of the β-boundary as shown in Fig. 3(d).

The above method can be applied to the edge states at the single-layer region. We consider the edge states at the left boundary in the left single region ($n = 0$) as an example. The boundary condition at $n = 0$ is given by

$$\begin{pmatrix} \Psi_{A_1,0} \\ \Psi_{B_1,0} \end{pmatrix} = \begin{pmatrix} 0 \\ \Psi_{B_1,0} \end{pmatrix}. \tag{B25}$$

This state can be the eigenvector of T only when $e_0 = 0$ and the eigenvalue of this eigenvector is a. Therefore, the edge states at the left boundary in the single-layer region exist only when $E = \epsilon_1$ and $|a| = |2\cos\frac{k_y}{2}| < 1$, as obtained in the previous section. The edge states at the right boundary can be similarly studied by considering the inverse matrix of T.

[1] A. H. Castro Neto, F. Guinea, N. M. R. Peres, K. S. Novoselov, and A. K. Geim, Rev. Mod. Phys. **81**, 109 (2009).

[2] K. S. Novoselov, A. K. Geim, S. V. Morozov, D. Jiang, M. I. Katsnelson, I. V. Grigorieva, S. V. Dubonos, and A. A. Firsov, Nature **438**, 197 (2005).

[3] Y. Zhang, Y.-W. Tan, H. L. Stormer, and P. Kim, Nature **438**, 201 (2005).

[4] V. P. Gusynin and S. G. Sharapov, Phys. Rev. Lett. **95**, 146801 (2005).

[5] Y. Hasegawa and M. Kohmoto, Phys. Rev. B **74**, 155415 (2006).

[6] M. Fujita, K. Wakabayashi, K. Nakada, and K. Kusakabe, J. Phys. Soc. Jpn. **65**, 1920 (1996).

[7] K. Nakada, M. Fujita, G. Dresselhaus, and M. S. Dresselhaus, Phys. Rev. B **54**, 17954 (1996).

[8] M. Kohmoto and Y. Hasegawa, Phys. Rev. B **76**, 205402 (2007).

[9] E. V. Castro, K. S. Novoselov, S. V. Morozov, N. M. R. Peres, J. M. B. L. dos Santos, J. Nilsson, F. Guinea, A. K. Geim, and A. H. C. Neto, Phys. Rev. Lett. **99**, 216802 (2007).

[10] E. V. Castro, N. M. R. Peres, J. M. B. Lopes dos Santos, A. H. C. Neto, and F. Guinea, Phys. Rev. Lett. **100**, 026802 (2008).

[11] K. A. Ritter and J. W. Lyding, Nature Mater. **8**, 235 (2009).

[12] C. Tao, L. Jiao, O. V. Yazyev, Y.-C. Chen, J. Feng, X. Zhang, R. B. Capaz, J. M. Tour, A. Zettl, S. G. Louie, H. Dai, and M. F. Crommie, Nature Physics **7**, 616 (2011).

[13] E. V. Castro, K. S. Novoselov, S. V. Morozov, N. M. R. Peres, J. M. B. L. dos Santos, J. Nilsson, F. Guinea, A. K. Geim, and A. H. C. Neto, Journal of Physics: Condensed Matter **22**, 175503 (2010).

[14] E. McCann and V. I. Fal'ko, Phys. Rev. Lett. **96**, 086805 (2006).

[15] E. McCann, Phys. Rev. B **74**, 161403 (2006).

[16] T. Ohta, A. Bostwick, T. Seyller, K. Horn, and E. Rottenberg, Science **313**, 951 (2006).

[17] J. B. Oostinga, H. B. Heersche, X. Liu, A. F. Morpurgo, and L. M. K. Vandersypen, Nature Materials **7** (2007).

[18] K. F. Mak, C. H. Lui, J. Shan, and T. F. Heinz, Phys. Rev. Lett. **102**, 256405 (2009).

[19] A. B. Kuzmenko, I. Crassee, D. van der Marel, P. Blake, and K. S. Novoselov, Phys. Rev. B **80**, 165406 (2009).

[20] Y. Zhang, T.-T. Tang, C. Girit, Z. Hao, M. C. Martin, A. Zettl, M. F. Crommie, Y. R. Shen, and F. Wang, Nature **459**, 820 (2009).

[21] Z. Q. Li, E. A. Henriksen, Z. Jiang, Z. Hao, M. C. Martin, P. Kim, H. L. Stormer, and D. N. Basov, Phys. Rev. Lett. **102**, 037403 (2009).

[22] E. V. Castro, N. M. R. Peres, and J. M. B. L. dos Santos, EPL (Europhysics Letters) **84**, 17001 (2008).

[23] J. Nilsson, A. H. Castro Neto, F. Guinea, and N. M. R. Peres, Phys. Rev. B **76**, 165416 (2007).

[24] T. Nakanishi, M. Koshino, and T. Ando, Phys. Rev. B **82**, 125428 (2010).

[25] J. W. González, H. Santos, M. Pacheco, L. Chico, and L. Brey, Phys. Rev. B **81**, 195406 (2010).

[26] Z.-X. Hu and W. Ding, ArXiv e-prints (2011), arXiv:1103.2754 [cond-mat.mes-hall].

[27] C. P. Puls, N. E. Staley, and Y. Liu, Phys. Rev. B **79**, 235415 (2009).

[28] E. V. Castro, M. P. López-Sancho, and M. A. H. Vozmediano, Phys. Rev. Lett. **104**, 036802 (2010).